Solvent effects on the ultrafast dynamics and spectroscopy of the charge-transfer-to-solvent reaction of sodide

Erik R. Barthel and Ignacio B. Martini
Department of Chemistry and Biochemistry, University of California, Los Angeles, California 90095-1569

Ernö Keszei
Department of Physical Chemistry, Loránd Eötvös University, Budapest, 1518 Budapest 112, P.O. Box 32, Hungary

Benjamin J. Schwartz[a)]
Department of Chemistry and Biochemistry, University of California, Los Angeles, California 90095-1569

(Received 27 September 2002; accepted 9 January 2003)

In ''outer sphere'' electron transfer reactions, motions of the solvent molecules surrounding the donor and acceptor govern the dynamics of charge flow. Are the relevant solvent motions determined simply by bulk solvent properties such as dielectric constant or viscosity? Or are molecular details, such as the local solvent structure around the donor and acceptor, necessary to understand how solvent motions control charge transfer? In this paper, we address these questions by using ultrafast spectroscopy to study a photoinduced electron transfer reaction with only electronic degrees of freedom: the charge-transfer-to-solvent (CTTS) reaction of Na^- (sodide). Photoexcitation of Na^- places the excited CTTS electron into a solvent-bound excited state; motions of the surrounding solvent molecules in response to this excitation ultimately lead to detachment of the electron. The detached electron can then localize either in an ''immediate'' contact pair (in the same cavity as the Na atom), which undergoes back electron transfer to regenerate Na^- in $\sim$1 ps, or in a ''solvent-separated'' contact pair (one solvent shell away from the Na atom), which undergoes back electron transfer in tens to hundreds of picoseconds. We present detailed results for the dynamics of each step of this reaction in several solvents: the ethers tetrahydrofuram, diethyl ether and tetrahydropyran and the amine solvent hexamethylphosphoramide (HMPA). The results are interpreted in terms of a kinetic model that both incorporates spectral shifting of the reaction intermediates due to solvation dynamics and accounts for anisotropic spectral diffusion in polarized transient hole-burning experiments. We find that the rate of CTTS detachment does not correlate simply with any bulk solvent properties, but instead appears to depend on the details of how the solvent packs around the solute. In contrast, the rate for back electron transfer of solvent-separated contact pairs varies inversely with solvent polarity, indicating a barrier to recombination and suggesting that this reaction lies in the Marcus inverted regime. For immediate contact pairs, the rate of recombination varies directly with solvent polarity in the ethers but is slowest in the highly polar solvent HMPA, suggesting that the spatial extent of the solvated electron in each solvent is one of the major factors determining the recombination dynamics. The fact that each step in the reaction varies with solvent in a different way implies that there is not a single set of solvent motions or spectral density that can be used to model all aspects of electron transfer. In addition, all of the results and conclusions in this paper are compared in detail to related work on this system by Ruhman and co-workers; in particular, we assign a fast decay seen in the near-IR to solvation of the CTTS p-to-p excited-state absorption, and polarization differences observed at visible probe wavelengths to anisotropic bleaching of the Na^- CTTS ground state. © *2003 American Institute of Physics.* [DOI: 10.1063/1.1557054]

I. INTRODUCTION

In recent years the development of tunable ultrafast laser sources has sparked a resurgence of interest in the study of charge-transfer-to-solvent (CTTS) reactions: the photodetachment of electrons from simple anions in solution.[1–4] Part of this interest centers on the fact that CTTS detachment provides an alternative mechanism to multiphoton ionization for the production of solvated electrons.[5] In addition, CTTS systems[6] represent the simplest condensed-phase photoinduced electron transfer reactions, and thus serve as models for understanding more complex electron transfer reactions found in biology and other fields.[7] From the considerable amount of theoretical work done on CTTS, the basic picture that has emerged is that the initially excited CTTS electron is bound by the polarization of the surrounding solvent and not by the solute from which it was detached.[8–11] Because the local environment is so strongly coupled to the CTTS excited

a)Author to whom correspondence should be addressed; Electronic mail: schwartz@chem.ucla.edu

state, CTTS reactions are outstanding candidates for the study of how solvation dynamics (the motions of solvent molecules in response to the movement of charge)[12] control electron transfer reactions. In particular, the use of atomic CTTS solutes without intramolecular degrees of freedom allows ultrafast spectroscopic experiments to directly monitor the motions of solvent molecules that drive electron transfer.[13]

The best known atomic CTTS transitions are those of the halides in water and in other polar solvents.[6] Bradforth and co-workers have extensively characterized the ultrafast dynamics of the CTTS reaction of aqueous iodide.[1] In their experiments, these workers used a UV laser pulse to excite the iodide CTTS transition and a near-IR pulse to monitor the detachment dynamics of the hydrated electron, which was observed to appear within 200 fs.[1] In addition to their work in aqueous solutions, Bradforth and co-workers also studied the CTTS dynamics of I^- in ethylene glycol and ethylene glycol/water mixtures.[1] As one might expect due to its high viscosity, the CTTS electron detachment dynamics were slower in ethylene glycol than in aqueous solution.[1] This suggests that bulk solvent properties such as viscosity are important in determining CTTS reaction dynamics. In addition, gas phase studies of I^-/water clusters by Neumark and co-workers have shown that much of the dynamical behavior of this system can be recovered in clusters where only the first solvent shell is present.[2] Together, these results suggest that while bulk solvent properties may facilitate much of the CTTS dynamics, motions of single solvent molecules in the first shell also substantially affect the CTTS process.

Our group also has explored the issue of how solvent motions control the dynamics of CTTS reactions.[13–15] Instead of focusing on aqueous halides, we have investigated the photophysics of another atomic CTTS solute, the sodium anion (Na^-, or sodide),

$$Na^- \xrightarrow{h\nu} Na^-{}^* \xrightarrow{\text{CTTS}} Na^0 + e^-_{\text{solvated}}.$$

To date, most of our studies have focused on the CTTS dynamics of Na^- in tetrahydrofuran (THF). However, sodide also can be prepared in a variety of other ether and amine solvents,[16] and in this paper we will take advantage of this fact to explore how solvent motions control the CTTS dynamics in this system. Like the halides, sodide has no internal vibrational or rotational degrees of freedom, so that any spectroscopic dynamics measured during the course of the CTTS reaction directly reflect the response of the solvent. In addition, sodide has the added bonus that *all* of the species in the reaction, the ground state CTTS absorption of the sodide reactant, the absorption of the CTTS excited state ($Na^-{}^*$) intermediate and the absorptions of the solvated electron and solvated sodium atom products, have well separated spectra and can be observed essentially independently,[13–15] as shown in Fig. 1. By taking advantage of the convenient spectroscopy of this system, we have constructed a molecular-level picture of how the local solvent motions determine the dynamics of the Na^- CTTS reaction.[13] In our picture, the initial absorption of a visible photon by Na^- creates the solvent-bound CTTS excited state, $Na^-{}^*$. At the instant of excitation, even through the CTTS electron is no longer bound to its Na atom parent, the solvent has not had time to solvate the underlying sodium atom core. Thus, CTTS excitation leaves the core in a gas phaselike environment, so that one spectroscopic manifestation of the CTTS excited state is a strong absorbance near 590 nm, reminiscent of the gas phase sodium D line (Fig. 1, circles). As time progresses, solvent motions lead to detachment and solvation of the excess electron, which absorbs near 2 μm (Fig. 1, dotted–dashed curve) on a time scale of $\sim$700 fs.[13]

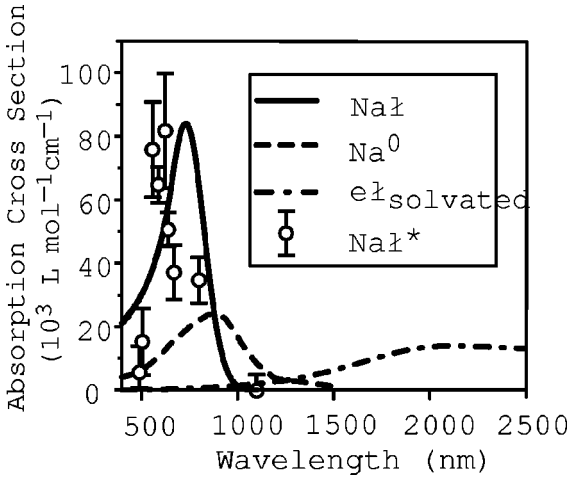

FIG. 1. Absorption spectra of the relevant spectroscopic species in the Na^- CTTS reaction in THF: Na^- (this work; solid curve); the CTTS excited state $Na^-{}^*$ (this work; circles); the species with stochiometry Na^0 (dashed curve; Ref. 19); the solvated electron e^-_{solvated} (dotted–dashed curve; Ref. 30). For the spectrum of $Na^-{}^*$, the error bars represent plus or minus one standard deviation.

Once the CTTS detachment is complete, we found that the back electron transfer reaction to regenerate Na^- takes place on one of three very different time scales, suggesting that the freshly detached CTTS electron can localize in one of three distinct spatial environments relative to its geminate sodium atom partner.[13–15] If the detached electron has the sodium atom in its first solvation shell (a species we refer to as an *immediate contact pair*), the direct overlap of the electron's wave function with its geminate Na^0 partner allows recombination to take place in $\sim$1 ps. If the detached electron localizes one solvent shell away from its Na^0 partner (a species we refer to as a *solvent-separated contact pair*[13–15]), however, back electron transfer cannot take place until an appropriate fluctuation disrupts the local solvent structure. For Na^- in THF at room temperature, these fluctuations occur infrequently, so that recombination takes place only on a hundreds-of-ps time scale.[13] Finally, if the electron localizes two or more solvent shells away from the sodium atom, it behaves in the same manner as an isolated solvated electron in the liquid (which we refer to as a *free solvated electron*). Free solvated electrons do not undergo recombination on sub-ns time scales, since their recombination is limited by diffusive encounters with their geminate Na^0 partners, nongeminate sodium atoms, or scavenging impurities.[13]

In addition to our studies, the dynamics of the CTTS reaction of Na^- in THF also has been investigated by Ruhman and co-workers.[17,18] Ruhman and co-workers' experi-

ments were performed with better time resolution (~50 fs) than our own (~200 fs), enabling these workers to see dynamical features that we had missed. First, Ruhman and co-workers observed a ~200 fs ''anomalous'' excess bleach of the Na^- ground state at wavelengths to the red of their excitation light. They assigned this feature to stimulated emission from the sodide CTTS excited state.[18] In combination with their observation of a similar ~200 fs decay in the 1200–1500 nm transient absorption, these workers proposed that the electron becomes detached within ~200 fs,[18] rather than on the ~700 fs time scale as we have argued.[13,14] Second, Ruhman and co-workers observed a polarization dependence in the bleach recovery of the Na^- ground state, suggesting that the Na^- absorption spectrum is inhomogeneously broadened.[17] These workers also found that the ~590 nm absorbing intermediate does not show any initial polarization anisotropy. Based on this, Ruhman and co-workers have asserted that the 590 nm absorbing species cannot be the initially excited CTTS state, since they expect both the excited CTTS electron and the 3*s* electron remaining on the Na atom core to carry the polarization memory of the initial excitation. Thus, unlike our assignment to the CTTS excited state,[13] these workers claim that the 590 nm absorbing species must be a post-ejection photoproduct—an unsolvated gas-phase-like Na atom that appears only after the electron ejection is complete.[17] Finally, these workers also noted that the 590 nm absorbing species shows a spectral shift to the blue at early times. In order to reconcile this blueshift with the ~700 fs appearance of the solvated Na^0 species at wavelengths in the near-IR (absorption maximum near 900 nm;[19] Fig. 1, dashed curve), Ruhman and co-workers have argued that solvent motions also cause detachment of the second valence electron from Na^-, so that the near-IR absorbing species with stoichiometry Na^0 is better thought of as a solvated sodium cation:solvated electron contact pair[17] rather than a solvated neutral sodium atom, as in our picture.[13]

Based on their results, Ruhman and co-workers take exception[17] to our picture of the Na^- CTTS reaction and to the kinetic model we have proposed[13] to describe its dynamics. In particular, these workers believe that inclusion of the spectral changes due to solvation of the various reaction intermediates is important to any description of the observed spectral dynamics in this system. Thus, in this paper, we test our understanding of the Na^- CTTS reaction and investigate the importance of solvation-induced spectral shifts by exploring the dynamics in a variety of solvents. We then present a new kinetic model that can successfully describe the reaction dynamics in multiple solvents. The new model is an extension of one we proposed previously,[13] with modifications to include solvation dynamics that account for spectral changes during the course of the reaction. The fact that our multisolvent data set is consistent with the model provides strong evidence that our basic picture of the dynamics in this system is correct, and also allows us to make rational assignments for the dynamical features seen throughout the spectrum for this model CTTS system. Of course, consistency of the data with any particular model does not constitute proof of the underlying mechanism. However, we will argue throughout this paper that our model is physically reasonable, and that it can describe all the data (both ours and that of Ruhman and co-workers[17,18]) for this system with relatively few adjustable parameters. We also will argue that there is no simple way to model this reaction using the picture proposed by Ruhman and co-workers: any kinetic scheme based on their picture would involve complex, three-body recombination and a large number of adjustable parameters. Thus, based on Occam's razor and the multisolvent data set presented here, we believe that the model presented below provides a correct basic description of the dynamics of the Na^- CTTS reaction.

In addition to providing new insights into the molecular picture underlying CTTS dynamics, our primary reason for studying the sodide CTTS reaction in different solvents is to understand how CTTS dynamics are affected by properties such as solvent viscosity, solvent polarity and local solvent structure. We find that rates of each of the elementary processes in the Na^- CTTS reaction—the initial electron detachment, dynamic solvation, the recombination of immediate contact pairs, and the recombination of solvent-separated contact pairs—depend on the choice of solvent in a different way. For example, the back electron transfer rate for solvent-separated contact pairs varies inversely with the solvent polarity, while the back electron transfer rate for immediate contact pairs does not scale simply with any bulk solvent parameters but instead appears to depend on how well the detached electron is localized by the solvent. The rate for the CTTS electron detachment also does not vary with bulk solvent parameters in a simple way, but correlates with the details of how the solvent packs around the ground state anion. The fact that each of these dynamical process varies with solvent in a different way suggests that different solvent motions are responsible for each step of the reaction. This means that there is no simple way to rationalize all the reaction dynamics using a single spectral density or spectrum of couplings.[20] Instead, understanding the molecular details of how the motions of the surrounding solvent molecules couple to the reactants is critical to determining how the solvent controls the dynamics of electron transfer reactions.

II. EXPERIMENT

The sodide solutions used in this study were prepared by a modification of the technique of Dye;[16] the details have been described previously.[14] Briefly, for solutions in tetrahydrofuran (THF), small amounts of Na and K metal were placed in a homebuilt sealed 1 mm path length spectrophotometer cell along with ~1 mL of a 1:400 v/v 15-crown-5 ether/THF solution. The samples were then agitated via sonication, and diluted with dry THF until an optical density of ~2 at the 730 nm absorption maximum was obtained. For solutions in the ethers tetrahydropyran (THP) and diethyl ether (DEE) [see Fig. 2(B) for the chemical structures of the solvents used in this work] we found that the use of 18-crown-6 ether produced more stable Na^- solutions than 15-crown-5.[21] Thus, the DEE and THP solutions were prepared by first adding chunks of the two metals to ~1 mL of neat dry solvent, and then adding one or two submilligram crystals of 18-crown-6 directly to the spectrophotometer cell.

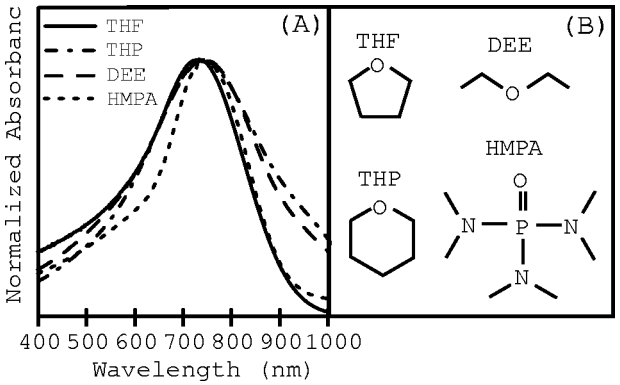

FIG. 2. (A) Absorption spectra of Na^- in the solvents THF (solid curve), DEE (dashed curve), THP (dotted–dashed curve), and HMPA (dotted curve). (B) Chemical structures of each of the four solvents used in this study.

The slightly larger cavity size of 18-crown-6 relative to 15-crown-5, however, resulted in an unavoidable slight increase in dissolved K^-, as evident in the red tails in the absorption spectra shown in Fig. 2(A). To minimize any effects of K^- contamination in our data, we chose pump and probe wavelengths to minimize any dynamical contributions from this species. All samples were used as directly prepared for the experiments, although in some cases dilution with additional freshly distilled dry solvent was required. All the Na^-/ether samples were stable for weeks if stored in the dark at $-20\,°C$.

We also prepared sodide solutions in the amine solvent hexamethyl phosphoramide (HMPA). Sodium metal readily disproportionates into Na^- and Na^+ in this solvent without the need for cation-complexing agents such as crown ethers.[16] The dissolution of Na metal is so favored in HMPA that it was difficult to prepare solutions with a low enough optical density to allow for spectroscopic transmission measurements. Thus, unlike the Na^-/ether solutions, the Na^-/HMPA solutions were prepared in a sealed 0.1 mm (100 μm) path length cell.[22] We found that the Na^-/HMPA samples typically were stable for only $\sim$1 day following preparation. We note that the dissolution of sodium in HMPA also produces solvated electrons as well as Na^- at equilibrium;[23] the contribution of these electrons to the pump–probe signals was eliminated by digitally locking the detection to the frequency of the chopped excitation beam.[24]

The photon source used for these experiments is a regeneratively amplified Ti:sapphire laser [Spectra Physics] producing $\sim$120 fs pulses at 780 nm with a 1 kHz repetition rate. The amplified beam pumps a dual-pass optical parametric amplifier (OPA) that produces tunable infrared signal and idler beams; these beams were used directly to probe transient absorptions between 1.2 and 2.4 μm. For some experiments, the IR signal and idler beams also were sum-frequency mixed with the 780 nm fundamental beam in an additional BBO crystal to produce visible pulses between 460 and 600 nm. These visible pulses were used both for pumping the sodide CTTS transition and for probing the Na^- ground state bleaching dynamics.[25] Even though the Na^-/ether samples tended to degrade over the course of several weeks, we did not detect any changes in the dynamics as a function of sample concentration or aging. All of the experiments presented here were performed at room temperature. As in our previous work,[14] we did not observe a significant dependence on the relative polarization of the pump and probe pulses for any of the data collected in THF or DEE, a result consistent with the observations of Ruhman and co-workers,[17] who found that the polarization anisotropy of Na^- in THF persists for times comparable to or less than our $\sim$200 fs instrumental resolution. We were able, however, to observe a polarization dependence similar to that of Ruhman and co-workers in THP, where the solvent dynamics are slow enough that the anisotropy persists for times longer than our instrument response, as discussed in more detail in Sec. IV B.

III. RESULTS AND KINETIC MODEL

A. Steady-state and pump–probe spectroscopy of Na^- in different solvents

Figure 2(A) shows the CTTS absorption band of Na^- in the ether solvents tetrahydrofuran (THF), diethyl ether (DEE) and tetrahydropyran (THP), as well as in the nonether solvent hexamethylphosphoramide (HMPA). Figure 2(B) shows the chemical structures and Table I lists the static dipole moment, dielectric constant, and viscosity of each of the four solvents used in this study.[26–28] Figure 2(A) shows that in spite of the large variation in solvent properties, the absorption band of Na^- is very similar in all four solvents. While this similarity is not surprising for the three ethers, it is somewhat unexpected for highly polar HMPA. The lack of a substantial solvatochromic shift of Na^- in HMPA can be attributed to the rather diffuse nature of the positive end of the HMPA dipole, which is distributed over all six methyl groups of the molecule and thus cannot interact strongly with the sodium anion.[29] It also is possible that steric interactions prevent the first-shell HMPA molecules from getting close

TABLE I. Bulk properties of the solvents used in this work.

Solvent	Abbreviation	n[a]	$\varepsilon/\varepsilon_0$[a]	μ (Debye)[a]	η (mPa s)
tetrahydrofuran	THF	1.406	7.47	1.75	0.456[b]
tetrahydropyran	THP	1.42	5.68	1.63	0.8008[c]
diethyl ether	DEE	1.352	4.42	1.15	0.224[b]
hexamethylphosphoramide	HMPA	1.458	29	5.55	

[a]From Ref. 26.
[b]From Ref. 27.
[c]From Ref. 28.

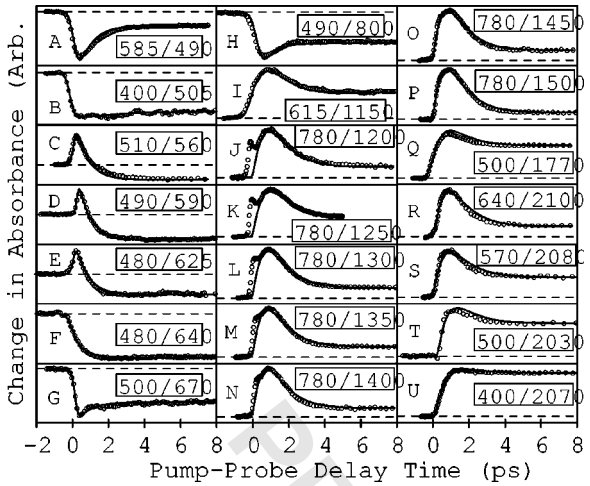

FIG. 3. Partial pump–probe data set for Na^- in THF. The circles show the experimentally measured data, while the solid lines are fits to the DE+S model; see text for details. The data are organized in order of increasing probe wavelength, with the excitation and probe wavelengths indicated in the legends given in nanometers. The data in panels (A), (C)–(E), (G)–(I), and (R)–(U) have been presented previously in Ref. 14; all the other data are new to this work.

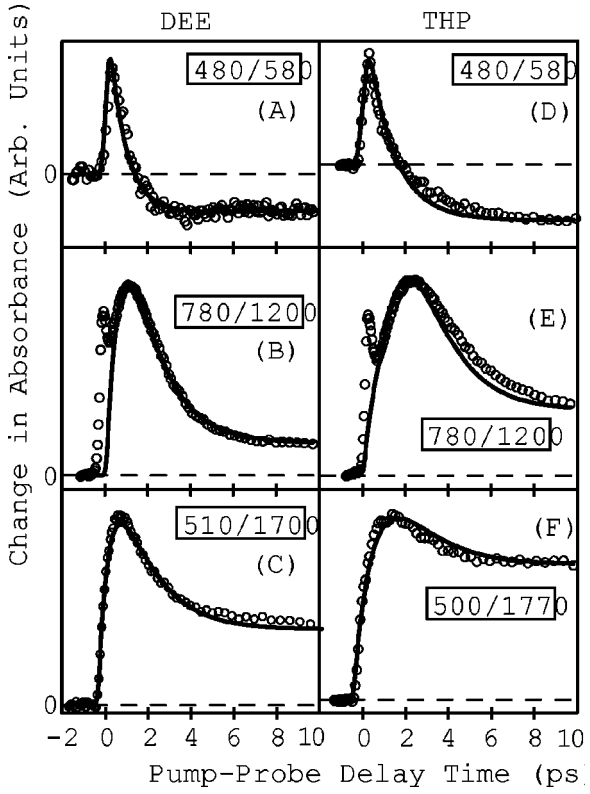

FIG. 4. Representative pump–probe data for Na^- in DEE (left panels) and THP (right panels). The circles are the experimental data, while the solid lines are fits to the DE+S model; see text for details. The excitation and probe wavelengths indicated in the legends are in nanometers.

enough to Na^- to provide the same type of stabilization that could be achieved by a less bulky molecule with the same dipole moment.

The circles in Fig. 3 show part of a typical short-time pump–probe data set for Na^- in THF, with probe wavelengths throughout the visible Na^- CTTS band [panels (A)–(H)], on the red side of the Na^0 absorption [panel (I)], in the 1250–1500 nm region [panels (J)–(P)], and near the solvated electron's $\sim 2\,\mu$m absorption maximum [panels (Q)–(U)]. For the visible-probe scans, the rise of the transient bleach in Fig. 3(A) is instrument limited, indicating that the Na^- ground-state absorption at 490 nm is lost as fast as the anion can be excited at 585 nm. The bleach then recovers on a ~ 1 ps time scale from the creation of new sodium anions via the recombination of immediate contact pairs. The offset remaining at longer times indicates that not all the detached electrons undergo rapid back electron transfer, since some are localized farther from the Na atom in solvent-separated contact pairs or as free electrons. Figures 3(C)–3(E) show the instrument-limited appearance of a transient absorption for probe wavelengths near 590 nm. The intensity and spectral position of this absorption are reminiscent of the Na D-line, suggesting that unsolvated Na atoms are formed within the instrumental resolution (cf. Fig. 1, circles). As the bare Na atom becomes solvated and CTTS detachment takes place, this absorption disappears in ~ 700 fs, leaving a bleach due to the loss of sodium anions. Near the peak of the CTTS absorption band, the data in Figs. 3(G) and 3(H) show dynamical signatures similar to those seen in Fig. 3(A). The traces in Figs. 3(G) and 3(H) have higher long-time offsets than that in Fig. 3(A) due to the use of more energetic pump wavelengths, which produce higher fractions of solvent-separated contact pairs and free solvated electrons; this effect of higher offsets with more energetic pump wavelengths can also be seen when probing the solvated electron near 2 μm in Figs. 3(Q)–3(U).[14,15] In the infrared, Fig. 3(I) shows the transient dynamics at 1150 nm, a wavelength that probes primarily the dynamics of the solvated Na atom (cf. Fig. 1, dashed curve).[13,14,19] The data show a ~ 700 fs rise, indicating the delayed appearance of fully solvated Na^0, and then a ~ 1 ps decay due to the recombination of the solvated Na atoms in immediate contact pairs. The data in Figs. 3(J)–3(P) show complex transient dynamics in the 1200–1500 nm region, where both the solvated Na atom and the solvated electron absorb. After an initial instrument-limited rise, there is a fast (~ 200 fs) decay followed by a slower ~ 700 fs rise and subsequent ~ 1 ps decay. The relative amplitude of the instrument-limited rise and fast decay decreases as the probe wavelength is tuned to the red. Ruhman and co-workers also have observed similar kinetics in this spectral region;[17,18] we will discuss our assignment of the various dynamical features below in Secs. IV A and IV C. Finally, the data in Figs. 3(Q)–3(U) show the transient dynamics associated with the solvated electron near its $\sim 2\,\mu$m absorption maximum.[30] The traces are qualitatively similar to the 1150 nm trace probing the Na^0 in Fig. 3(I), showing a delayed appearance of solvated electrons followed by a ~ 1 ps decay due to the recombination of electrons in immediate contact pairs and an offset from the electrons that have not yet recombined. The fact that the absorptions of both Na^0 and the solvated electron disappear on the same time scale as the bleach recovery of Na^- verifies that the ~ 1 ps kinetic feature we observe in all the scans is due to a back electron transfer reaction.[13,14]

The circles in Fig. 4 show a representative subset of similar pump–probe data sets for Na^- in DEE (left panels)

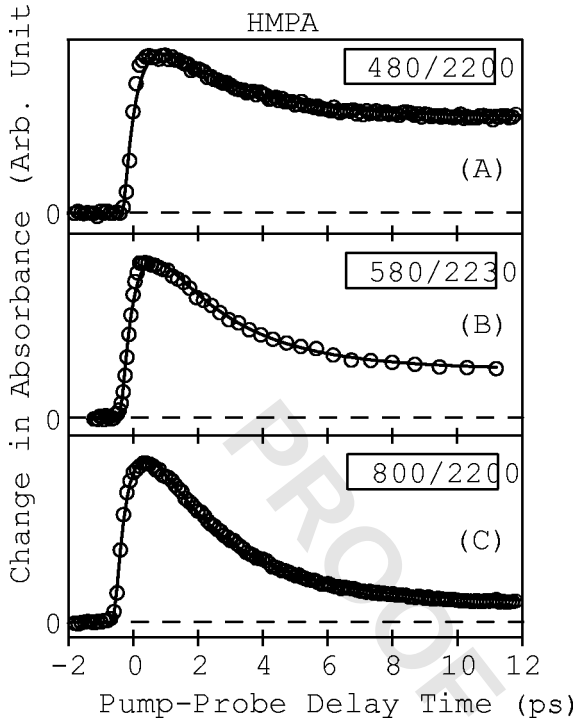

FIG. 5. Pump–probe data set for Na^- in HMPA. The circles are the experimental data; the solid lines are fits to the DE+S model (without the inclusion of solvation of Na^0); see text for details. Excitation and probe wavelengths indicated in the legends in nanometers.

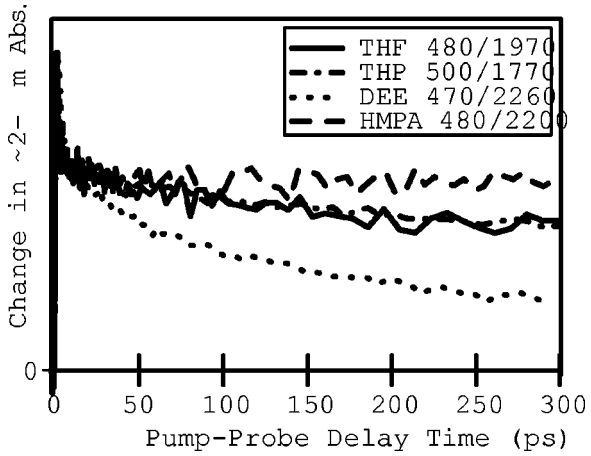

FIG. 6. Transient absorption dynamics of the solvated electron on a ~300 ps time scale following CTTS excitation of Na^- in each of the solvents whose chemical structures are shown in Fig. 2. The data are scaled to have the same value at a time delay of 11 ps for ease of comparison. Excitation and probe wavelengths (in nm) are indicated in the legend.

and THP (right panels). The data in DEE and THP are qualitatively similar at each pump/probe wavelength combination to those in THF, but the selected scans in the figure makes it clear that there are differences in the CTTS dynamics of Na^- between the three solvents. For example, close inspection reveals that the traces with IR probe wavelengths have completed their short-time dynamics and reached their plateau values by ~4 ps in THF, but take 6 to 8 ps in DEE and THP, which in our picture reflects a change in the time scale for the back electron transfer reaction from immediate contact pairs. In addition, the decay of the 590 nm absorbing species and the slow rise of the absorptions at 1200 and 1700 nm, which we assign to the time to detach the electron from the CTTS excited state, are similar in DEE and THF, but take ~50% longer in THP. Since the Na^- CTTS reaction has only electronic degrees of freedom, all of the observed differences in dynamics must be a direct reflection of the underlying motions of the solvent. The fact that the various dynamical features of the data do not all vary in the same manner as the solvent is changed indicates that different solvent motions must be responsible for each aspect of the dynamics involved in the CTTS excitation of Na^-.

The circles in Fig. 5 show a limited set of pump–probe data for Na^- in HMPA. The data set is restricted to probe wavelengths in the ~2-μm region where the solvated electron absorbs due to difficulties with controlling the concentration of the sample.[22] The long-time offsets in the data show the same trend with excitation wavelength as in the ethers: at more energetic excitation wavelengths, fewer electrons are ejected into immediate contact pairs, resulting in higher offsets at longer times. It is also clear that the signals in HMPA decay more slowly than in any of the ethers, implying that the recombination of immediate contact pairs is much slower in this solvent. In addition, the rise of the solvated electron's absorption in HMPA is quite a bit faster than in the ethers, suggesting either more rapid detachment of the electron from the CTTS excited state, or as will be discussed further below, the presence of an excited-state absorption in the ~2 μm spectral region. Thus, even though the dynamics are qualitatively similar in the ethers and HMPA, there are no simple trends as to which time scales increase and which decrease in the amine-based solvent relative to the ethers.

Finally, Fig. 6 displays scans on the hundreds-of-ps time scale in which the Na^- CTTS band was excited at ~480 nm and the dynamics of the detached electrons were probed near ~2 μm in each of the four solvents considered in this work; the traces are normalized at a time delay of 11 ps to facilitate comparison of the long-time dynamics. In our picture, these long-time dynamics reflect the back electron transfer of electrons trapped in solvent-separated contact pairs. We have argued in previous work that this long-time back electron transfer is not diffusion controlled,[14] and indeed, we see no correlation between the long-time back electron transfer rate and solvent viscosity. Instead, the rate at which this long-time back electron transfer takes place is highly sensitive to the solvent polarity: the recombination of solvent-separated contact pairs is fastest in the least polar solvent, DEE, and slowest in the most polar solvent, HMPA. Overall, the fact that some of the CTTS reaction time scales are faster in HMPA than the ethers and some are slower emphasizes that different molecular solvent motions are responsible for controlling the different mechanistic steps in this simplest of charge transfer reactions.

B. A new kinetic model for the CTTS reaction of Na^-

To obtain a quantitative understanding of how different solvent motions control the various processes in the CTTS detachment of electrons from Na^-, we need to fit the data to a kinetic model: simply fitting the data to sums of exponen-

tials does not guarantee consistency with any proposed underlying mechanism(s) and cannot provide a way to distinguish between processes that occur on similar time scales. Thus, we present in this section a new kinetic model that is consistent with the data presented in Figs. 3–5. The model presented here is an extension of the ''delayed ejection'' (DE) model that we had presented previously to describe the dynamics of the Na^- CTTS reaction in THF.[13] In our original DE model, photoexcitation of Na^- is assumed to create a CTTS excited state (Na^-*) from which solvent motions cause the excited electron to detach into an immediate or solvent-separated contact pair. Following detachment, the DE model further assumed that the newly detached e^-_{solvated} and its geminate Na^0 partner each appear instantaneously with their equilibrium absorption spectra. As we[13,14] and others[17] have pointed out, this approach provides only a ''zeroth order'' picture of the kinetics of the Na^- CTTS system since it neglects the effects of solvation dynamics on the spectroscopy of the photoproducts that are clearly manifest in pump–probe data. Thus, in the present model, we have added the possibility of solvation dynamics of the neutral sodium atom as it appears after CTTS. We also have allowed for a more realistic picture of how the ejected electrons are initially distributed following CTTS from sodide: the new model distinguishes between electrons that detach into immediate (subscript im) and solvent-separated (subscript sep) contact pairs, and those that become free electrons.

The new model, which we call the delayed ejection plus solvation (DE+S) model, is given by the following kinetic equations.

Photoexcitation,

$$Na^- \xrightarrow{h\nu} Na^-*. \tag{1}$$

CTTS detachment,

$$Na^-* \xrightarrow{\text{CTTS};\tau_1;p} (Na^0_{\text{HOT}}\cdot e^-_{\text{solvated}})_{\text{im}}, \tag{2}$$

$$Na^-* \xrightarrow{\text{CTTS};\tau_1;q} (Na^0_{\text{HOT}}\cdot e^-_{\text{solvated}})_{\text{sep}}, \tag{3}$$

$$Na^-* \xrightarrow{\text{CTTS};\tau_1;r} Na^0_{\text{HOT}} + e^-_{\text{solvated}}. \tag{4}$$

Solvation dynamics,

$$[Na^0]^{\text{total}}_{\text{HOT}} \xrightarrow{\text{solvation};S(t_1,t_2)} [Na^0]^{\text{total}}_{\text{equilibrium}}. \tag{5}$$

Back electron transfer (recombination) of contact pairs,

$$(Na^0\cdot e^-_{\text{solvated}})_{\text{im}} \xrightarrow{\text{recombination};\tau_2} Na^-, \tag{6}$$

$$(Na^0\cdot e^-_{\text{solvated}})_{\text{sep}} \xrightarrow{\text{recombination};\tau_3} Na^-. \tag{7}$$

Dissociation of contact pairs and diffusive recombination,

$$(Na^0\cdot e^-_{\text{solvated}})_{\text{sep}} \xrightarrow{\text{dissociation};\tau_4} Na^0 + e^-_{\text{solvated}}, \tag{8}$$

$$Na^0 + e^-_{\text{solvated}} \xrightarrow{\text{diffusion};\tau(E)} Na^-, \tag{9}$$

In the DE+S model, the absorption of Na^0 first appears upon decay of the CTTS excited state, but its spectrum then shifts and broadens with simple exponential behavior, represented by $S(t_1,t_2)$ in Eq. (5). Equation (5) introduces the notation $[Na^0]^{\text{total}}$ to represent the total concentration of neutral Na atoms, independent of whether they are part of one of the two kinds of contact pairs [Eqs. (2) and (3)] or present as free solvated atoms [Eq. (4)]. In other words, Eq. (5) is equivalent to assuming that all Na atoms have the same absorption spectrum and solvation dynamics, whether or not they are part of a contact pair, as we have argued should be the case in previous work.[13,14] We also point out that the processes in Eqs. (7)–(9) occur too slowly to be evident on the $\leqslant$10 ps time scale examined in the data in Figs. 3–5, so only Eqs. (1)–(6) are needed to interpret these short-time experiments. The mathematical details of implementing the model can be found in E-PAPS.[31] Here, we point out only that the relevant kinetic parameters in Eqs. (1)–(6) are τ_1 (the CTTS electron detachment time), τ_2 (the immediate contact pair recombination time), and p (the fraction of electrons ejected into immediate contact pairs). The photophysical parameters ε_{Na^-}, ε_{Na^-*}, ε_{e^-}, t_1, t_2, and $\varepsilon_{Na}(\omega,t)$ correspond to the absorption cross sections of sodide, the CTTS excited state, and the solvated electron, the times over which the Na^0 spectrum changes due to solvation, and the instantaneous Na^0 absorption spectrum at time t, respectively.

In the form given by Eqs. (1)–(6), the DE+S model uses static absorption spectra for the Na^-* CTTS excited state, the solvated electron, and the bleach of Na^-; solvation dynamics produce a shift only of the Na^0 spectrum. It would be straightforward to expand the model to include features such as the dynamic solvation of Na^-*, but since such processes are expected to occur on time scales comparable to or faster than our instrument resolution,[17,18] their inclusion would result only in the introduction of unnecessary parameters. We also can extend the model to include the effects of anisotropic hole burning (spectral diffusion in the polarized ground state bleach), and we will argue below in Sec. IV B that such modifications allow us not only to describe the polarized pump–probe scans that we have measured in THP (Fig. 9, below) but also the polarized data measured by Ruhman and co-workers in THF.[17] Thus, with only simple modifications, the DE+S model can be made consistent with all the known ultrafast pump–probe data for the Na^- CTTS transition.

One limitation in applying the DE+S model to data sets in multiple solvents is that the absorption spectra of many of the important kinetic species are not available in every solvent. For example, the absorption spectrum of the solvated electron is not available in THP, and the spectrum of the solvated neutral Na atom is available only in THF.[32] Therefore, in implementing the DE+S model, we have assumed that the spectra of solvated Na^0 and the solvated electron in THP and DEE are identical to that in THF. We believe that this is a reasonable assumption, since as shown in Fig. 2, the absorption spectrum of Na^- is very similar in these solvents, as is the spectrum of the solvated electron (Fig. 1, dotted–dashed curve in THF) in the solvents for which it is known.[33] With these assumptions, we are able to globally fit the model

TABLE II. Estimated DE+S model parameters (with 95% confidence intervals).

Solvent	τ_1 (ps)[a]	τ_2 (ps)[a]	t_1 (ps)[a]	t_2 (ps)[a]
THF	0.70±0.06	0.78±0.07	1.37±0.8	2.43±0.6
THP[b]	1.26	1.38	0.60	2.02
DEE	0.82±0.21	1.53±0.25	1.79±0.90	1.53±3
HMPA[c]	0.41±0.02	2.51±0.04	—[c]	—[c]

[a]τ_1 and τ_2 are the forward and reverse electron transfer times, respectively, for the Na^- CTTS reaction, while t_1 and t_2 are the wavelength maximum and spectral width/oscillator strength shifting times, respectively, for the Na^0 spectrum; see text for details.
[b]Errors for THP could not be estimated; see text for details.
[c]Solvation dynamics were not modeled in HMPA; see text for details.

to the data in Figs. 3–5, thereby providing a quantitative means to compare the results from the different solvents.

C. Fitting the model to the CTTS dynamics of Na^- in different solvents

The solid curves in Figs. 3–5 are global fits of the data in each solvent to the DE+S model, Eqs. (1)–(6). The global fits include 22 pump–probe scans in THF (the 21 scans shown in Fig. 3 plus a scan probing at 1900 nm), 14 scans in DEE and 13 scans in THP (for which three scans each are shown in Fig. 4), and the three HMPA scans in Fig. 5. The fitting parameters were estimated using a least squares reconvolution method.[34] This procedure included the calculation of the ''instantaneous'' signal, given by Eq. (S1) of E-PAPS, convolution with the instrument response function, and determination of the differences between the measured and convolved simulated data.[31] The sum of the squares of the differences was minimized using a Marquardt algorithm.[35] The procedure comprised a global fit for all measured kinetic curves at different excitation and detection wavelengths for each solvent. Kinetic parameters were global, while spectral parameters and pulse parameters were different for each wavelength. Though the instrument response function could be measured experimentally, in most cases, the effective pulse width parameters were also adjusted in the Marquardt procedure to get a better fit of the model (for more details, see Ref. 31). The estimated parameters obtained through this fitting procedure are shown in Table II. We note that we were unable to estimate the error for the values in THP, possibly due to a very shallow minimum in the parameter space that lead to little change in the final estimated parameters but large fluctuations in the estimated errors.

During parameter estimation, the forward (τ_1) and reverse (τ_2) ET times, and the Na^0 shifting and broadening time (t_1) and spectral area growth time (t_2), were constrained to be the same for all the scans from a given solvent. The absorption cross section of the CTTS excited state Na^-* was individually adjusted for each probe wavelength. For probe wavelengths in the IR ($\lambda_{probe} \geqslant 800$ nm), however, the Na^-* cross sections were found to be zero during the parameter estimation. Thus, in the fits presented in Figs. 3 and 4, we set the Na^-* cross sections at these wavelengths to zero to diminish the total number of adjustable parameters. Additional parameter constraints were placed on data that were obtained by exciting at the same wavelength [e.g., Figs. 3(C)–3(H), 3(Q), and 3(T), all of which show traces with ~500 nm excitation light]: these scans were forced to have the same value of p, the fraction of electrons that detach into immediate contact pairs instead of into solvent-separated contact pairs or free electrons.[36]

Given all the constraints, the total number of fitting parameters in the DE+S model for each data set, aside from the zero of time and an instrument response width parameter, is 23 for THF, 17 for THP, 15 for DEE, and 5 for HMPA, consisting of the forward and fast reverse electron transfer times τ_1 and τ_2, the recombination fraction p for each excitation wavelength,[36] the Na^0 spectrum solvation shifting parameters t_1 and t_2, the full widths at half-maximum on the Gaussian and Lorentzian sides of the Na^0 band, the amplitude of the Na^0 absorption at time zero, and the Na^-* excited state absorption cross sections at probe wavelengths $\leqslant 800$ nm. This means that on average, there are $\leqslant 1.2$ adjustable parameters for each pump–probe scan shown in Figs. 3 and 4. This is substantially fewer adjustable parameters than would have resulted from simple biexponential fits to each scan (which would have required three parameters, an amplitude ratio and two time constants, per scan). Of course, a simple biexponential function would neither be capable of fitting the wide range of time scales and long-time offsets in each scan, nor provide a test of any underlying reaction mechanism. The main point is that the DE+S model, despite its apparent complexity, is highly constrained, so that the quality of the fits seen in Figs. 3–5 argues that the underlying mechanism is consistent with the observed data in all four solvents.[37]

IV. DISCUSSION

The fits of the DE+S model to the data in Figs. 3–5 provide a quantitative means to compare how the different elementary processes in the Na^- CTTS reaction are affected by changing the solvent. The fitting parameters for the data in all four solvents, summarized in Table II, show that the forward electron transfer (CTTS) times (τ_1) increase in the order HMPA, THF, DEE, and THP. The immediate-pair back electron transfer (geminate recombination) times (τ_2) increase in the order THF, THP, DEE, HMPA, in order of decreasing polarity for the ethers but with HMPA as an anomaly. The broadening times for solvation of the sodium atom (t_1) in the ethers increase in the order DEE, THP, and THF, correlating with polarity in the opposite direction as for geminate recombination (solvation times are not available in HMPA since the probe wavelength range was limited only to the absorption of the solvated electron).[22] While the DE+S model fits the data remarkably well, it does not do so perfectly. Thus, before investigating the trends of how the fitting parameters vary with solvent, we start by discussing the implications for the places where the model does not adequately describe the data.

A. Assignment of the early-time feature in the 1200–1500 nm region

As seen in Figs. 3 and 4, the DE+S model fits most of the Na^- CTTS pump–probe scans quite well, but is unable

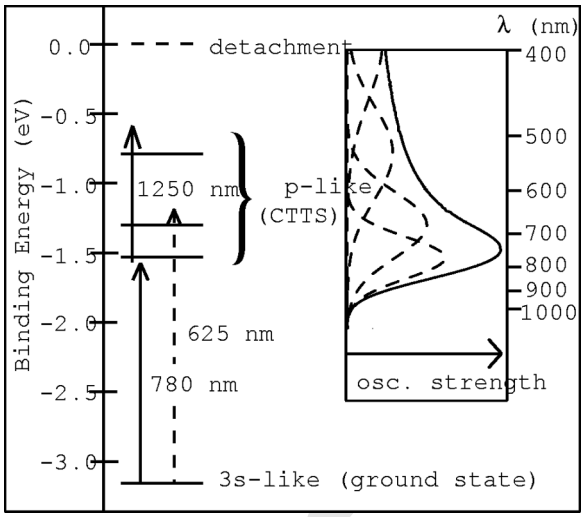

FIG. 7. Simple model for the electronic structure of Na^- assuming that the CTTS band consists of transitions from the sodide 3*s* orbital to three solvent-supported *p*-like states plus the continuum. The inset shows the experimental absorption band (solid curve) and the four Gaussian (in energy) bands comprising the fit (dashed curves). The main figure shows the positions of these bands on an absolute energy scale assuming that direct detachment occurs at ~400 nm (3.1 eV). The arrows show the relevant transitions for sodide if 780 nm pump and 1250 nm probe pulses are used (solid arrows), or if a 625 nm pump pulse is used (dashed arrow).

to account for the early time absorption feature in the ~1200–1500 nm region [panels (J)–(P) in Fig. 3, panels (B) and (E) in Fig. 4]. Thus, when fitting the model in this wavelength range, we excluded the data points between −1 and ~0.5 ps from the fit. In all the solvents, the feature that the model fails to describe in this wavelength range consists of a transient absorption with an instrument-limited rise that subsequently decays in ~200 fs. This feature was first seen in pump–probe experiments on Na^- in THF by Ruhman and co-workers,[17,18] and this feature clearly cannot be satisfactorily explained by Eqs. (1)–(6) in the DE+S scheme shown above.

Our rationalization for the origin of this early-time absorption feature is based on a consideration of the electronic structure of sodide. The anisotropic polarized bleaching dynamics observed by Ruhman and co-workers[17] suggest that the sodide CTTS absorption band likely consists of three transitions from the Na^- 3*s* ground state to *p*-like solvent-supported CTTS excited states, as discussed in more detail in Sec. IV B. If the solvent environment were perfectly spherical, the three *p*-like excited states would be degenerate; the fact that the local solvent environment is asymmetric breaks the degeneracy of these states.[17,18] In fact, we believe that there is a close analogy between the spectroscopy of the Na^- CTTS absorption band and that of the hydrated electron.[38,39] To get a rough idea of the underlying electronic structure, we modeled the ground state CTTS absorption as the sum of four Gaussian sub-bands (three *p*-like excited states and the continuum). Figure 7 shows the energies of the centers of each of these sub-bands, while the inset shows the shape of the experimental absorption spectrum and the resulting fit. The splitting between the lowest and highest of the *p*-like excited states is ~1 eV, corresponding to a wavelength near 1250 nm. Thus, based on this simple fitting procedure, we would expect the Franck–Condon absorption from the lowest CTTS excited state to occur in the near IR around 1250 nm.[40] We also expect this absorption to be quite weak: a true *p*-to-*p* transition would be one-photon forbidden by symmetry, but the fact that the local solvent cavity is not perfectly spherical breaks the symmetry, so that this distorted *p*-to-distorted-*p* transition is weakly allowed, as observed experimentally.[41] Thus, we can rationalize the instrument-limited appearance of an absorption in this spectral region as a manifestation of the CTTS excited state, an assignment in agreement with that of Ruhman and co-workers.[18]

Now that we can account for the existence of the instrument-limited absorption in this spectral region, the next question to ask is why does this absorption decay on a ~200 fs time scale? Ruhman and co-workers believe that this decay reflects a loss of population of the CTTS excited state, so that the CTTS detachment occurs on this time scale.[17,18] While this assignment is reasonable, the assumption of a fast electron ejection time makes it difficult to explain the subsequent ~700 fs rise of the signal at these wavelengths, which we assign to the appearance of solvated electrons and solvated Na atoms due to CTTS detachment with time scale τ_1 [Eqs. (2) and (3)]. The way Ruhman and co-workers rationalize this ~700 fs absorption rise is to assume that a second electron detaches from the Na atom core, producing a sodium cation:solvated electron contact pair[18] in addition to the original CTTS-detached electron. We believe that the possibility of ejecting a second electron is remote for three reasons. First, it is difficult to rationalize the recovery of the Na^- ground-state bleach only ~1 ps after CTTS excitation, since this would require a three-body recombination event involving two detached electrons and a sodium cation. Second, in previous work, we showed that re-excitation of the solvated electron at ~2 μm (a wavelength where the electron in a Na^+:e^- contact pair would *not* absorb) leads to an instrument-limited production of Na^- through accelerated back electron transfer.[15] We do not believe that vertical excitation at 2 μm is capable of placing *two* electrons back onto a Na cation, especially since one of the two electrons does not absorb at this wavelength. Finally, even if the second electron were to detach to produce a Na^+:e^- contact pair, this electron would not absorb in the region near 1.5 μm [cf. Fig. 1, dashed curve with Figs. 3(N)–3(P)], so detachment of the second electron cannot be the explanation for the ~700 fs absorption rise measured in this wavelength range by both our group and Ruhman's group.[17] Thus, we believe that the rapid decay of the CTTS excited state absorption is not a signature of the CTTS excited-state lifetime.

Although we do not believe that the rapid decay of the 1200–1500 nm absorption feature reflects the excited-state lifetime, there is a way to rationalize these CTTS excited-state dynamics in the context of the DE+S model. Based on the analogy between the spectroscopy of Na^- and that of the hydrated electron, we expect solvation dynamics to alter both the oscillator strength and the energy of the CTTS excited-state absorption as the solvent responds to the CTTS excitation.[42] To get a better understanding of these dynamics, we subtracted our DE+S fits, which we believe account for

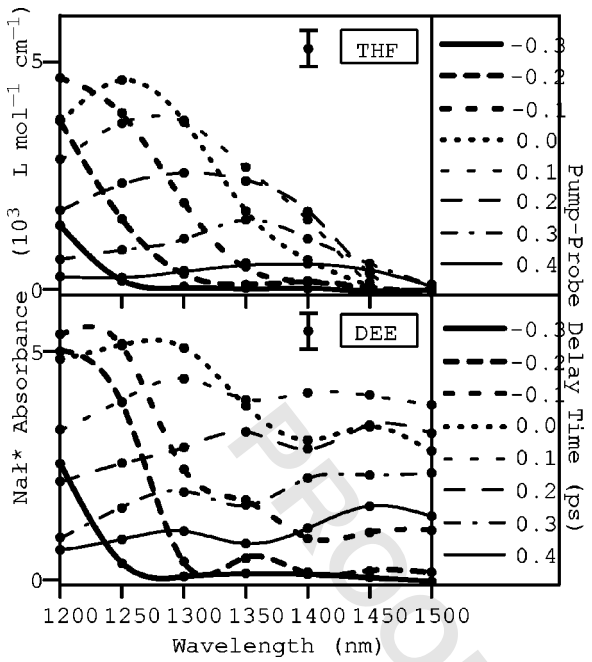

FIG. 8. Time and wavelength-resolved spectra of the short-time feature seen in panels (J)–(P) of Fig. 3 and similar data from DEE (not shown). The spectra were obtained by subtraction of DE+S fits data from the experimental data as described in the text. The points are shown with one standard deviation error bars; the curves are spline fits meant to guide the eye. The ordinate values for DEE could differ by a factor of ~1.5; see Ref. 33.

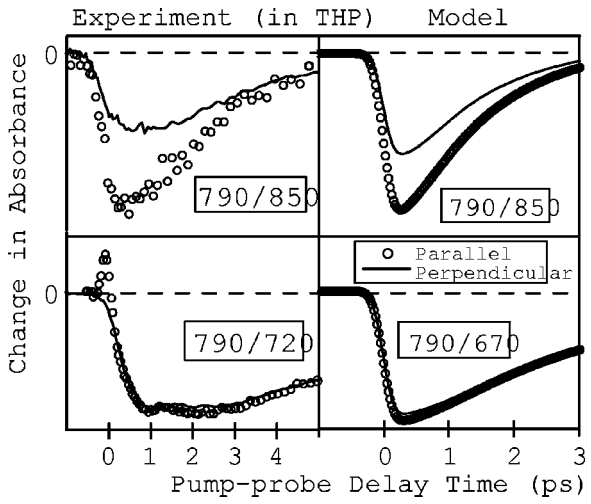

FIG. 9. Polarized transient absorption spectra of Na^- in THP. Circles represent a parallel pump–probe geometry, while solid lines represent the parallel geometry. Left panels, experimental data; right panels, simulations according to the DE+S model incorporating polarization of the sodide bleach presented in Ref. 31. Note that the probe wavelength was set in the simulation to 670 nm rather than the experimental value of 720 nm; see text and Refs. 44 and 45 for details.

all the other dynamical processes in the reaction, from the experimental data. This difference between the fits and the data, which is shown for both the THF and DEE data sets in Fig. 8, should reveal the dynamics of only the low-p-to-high-p CTTS excited-state absorption feature. This difference analysis shows that the short-lived feature in this spectral region does not simply decay, but also undergoes a large spectral shift to the red on a $\leqslant 0.5$ ps time scale in both solvents. We believe that this redshift makes sense: solvent motions should work to decrease the energy gap of the ~1250 nm p-to-p transition of Na^-* as part of its evolution toward becoming the $\sim 2\,\mu$m absorption of the solvated electron once detachment is complete. Thus, we assign the early time absorption decay in the 1200–1500 nm spectral region to a weak excited-state absorption that shifts rapidly to the red via solvation.

B. Polarization dependence and anisotropic bleaching

In addition to the rapid ~200 fs decay in the 1200–1500 nm spectral region, Ruhman and co-workers have observed a similar early time feature in Na^-/THF solutions in 800 nm pump/850 nm probe polarized bleach experiments.[17] Ruhman and co-workers have assigned the rapidly decaying component of the parallel–polarized bleach to stimulated emission from the CTTS excited state.[18] These workers also used this fast decay as support for their assignment that the similar rapidly decaying feature seen near 1200 nm is due to the detachment of the electron from Na^-*.[18] These workers also have argued, however, that the Na^- CTTS band is inhomogeneously broadened.[17] One manifestation of inhomogeneous broadening should be the appearance of an excess polarized bleach when the probe wavelength is tuned to the same polarization sub-band as the pump wavelength; this excess polarized bleach should decay rapidly as solvent fluctuations scramble the polarization of the bleached transition,[38,43] as discussed in more detail in Ref. 31. Indeed, Ruhman and co-workers' original assignment of their polarized pump–probe data was solely to anisotropic bleaching dynamics.[17] We were unable to observe this polarization dependence in our previous work on Na^-/THF solutions[14] because the difference between the parallel and perpendicularly polarized pump–probe dynamics decays on a time scale comparable to our time resolution.[17,18]

The data in Fig. 4 show that the dynamics of all aspects of the Na^- CTTS reaction are slower in THP than THF. This suggests that the solvent fluctuations responsible for anisotropic bleaching in this system are also likely to be slower, and thus should be observable with our ~200 fs time resolution. Indeed, Fig. 9 shows polarized transient absorption data on Na^- in THP for 790 nm pump/850 nm probe (top left panel) and 790 nm pump/720 nm probe (bottom left panel) experiments. Like Ruhman and co-workers,[17,18] we see a distinct polarization dependence when probing to the red of the pump: the parallel probe scan shows an excess bleach that decays in a few ps to become identical to the perpendicular probe scan. When probing to the blue side of the band, changing the relative polarizations of the pump and probe beams produces little effect. The question is, does the excess bleach seen in the parallel scan when probing to the red of the pump wavelength result from stimulated emission from the CTTS excited state, or can it be explained solely by anisotropic bleaching dynamics?

To address this question, we have simulated the anisotropic bleaching dynamics of Na^- by assuming that the underlying electronic structure is as in Fig. 7 and that spectral

diffusion occurs as a single monoexponential Poisson process; the details of our simulations (along with a spreadsheet to allow simulation of the data at any combination of pump and probe wavelengths for both parallel and perpendicular relative polarization) are given in Ref. 31. The basic idea is that an 800 nm polarized pump pulse excites only that subset of the Na^- species that have their lowest-energy transitions aligned along the laser polarization. A parallel–polarized probe beam in the same sub-band directly measures the depletion of this population, but a perpendicularly polarized probe beam does not, since members of the ensemble whose lowest-energy absorption is oriented orthogonal to the pump polarization still absorb at the probe wavelength. As solvent fluctuations scramble the direction of the transition dipoles of the excited subensemble, the distinction between parallel and perpendicular relative polarizations disappears. The upper right panel in Fig. 9 shows a simulation of the polarized 780/850 THP data using the parameters from the DE+S model summarized in Table II and a single additional parameter describing the anisotropic spectral diffusion time (set here to be 2.0 ps). The simulation qualitatively reproduces the data,[44] suggesting that anisotropic bleaching alone is sufficient to explain the observed polarization dependence.

Figure 7 shows that as the probe wavelength is tuned to the blue, it no longer interrogates only the sub-band that was originally excited but also measures the bleaching dynamics of the adjacent sub-band. If the probe is tuned to a wavelength near the crossing point of the two sub-bands, this will effectively negate any polarization dependence, as shown in the simulated data in the lower right panel of Fig. 9. The simulated data in this panel used all the same parameters as that in the upper panel, although the simulated probe wavelength was adjusted to sit nearer to the crossing point of the two sub-bands.[45] Clearly, the lack of polarization dependence when probing to the blue of the excitation wavelength can be explained within a model incorporating only anisotropic bleaching. In addition to reproducing the data in the left panels of Fig. 9, it is possible to use the spreadsheet presented in Ref. 31 to qualitatively reproduce all the high time resolution polarized data in THF presented by Ruhman and co-workers.[17,18] The small discrepancies between the simulated and experimental data easily could be accounted for by assuming a more complex functional form for the anisotropic spectral diffusion; the main point is that all the essential features of the polarized data can be captured with the addition of only a single parameter. Overall, while we cannot rule out stimulated emission as a partial source of the excess bleach, our model makes clear that it is unnecessary to include stimulated emission in order to describe the polarized pump–probe data from both our group and Ruhman's.

C. Connection between the 1250 nm and 590 nm transiently absorbing species

While we can adequately explain the transient spectroscopy of Na^- using the DE+S model plus anisotropic spectral diffusion, one question that deserves further scrutiny is why the solvent shifting time of the near-IR transient feature (Fig. 8), which we assign to the p-to-p CTTS-excited state, does not match the decay time of the 590 nm absorbing photoproduct, which we also assign as arising from Na^-*. We believe that the 590 nm feature is the D-line absorption of the Na atom core, which is in a gas phaselike environment because it is shielded from the solvent by the yet-to-be-detached excited electron.[13] It makes sense that the early-time solvation processes would affect the directly exposed excited CTTS electron to a greater extent than the shielded core. Thus, the solvent response to the CTTS excitation causes a rapid redshift and change in oscillator strength of the p-to-p excited-state transition, but the Na atom core remains isolated from the solvent until after it is exposed by detachment of the excited electron.[46] The small dynamic blueshift of the 590 nm absorbing feature observed by Ruhman and co-workers[18] and the large redshift of the 1250 nm absorbing feature seen in Fig. 8 provide further evidence that solvation dynamics can have different effects on the Na atom core and CTTS excited-state absorptions.

Our view of both the ~1250 nm and ~590 nm absorptions as providing different manifestations of the CTTS excited state requires considering the details of how the CTTS transition occurs. While Na^- is best thought of as a two-electron system, preliminary results from mixed quantum-classical simulations in our group suggest that the CTTS transition has essentially one-electron character: the calculated multielectron CI wave function of the CTTS excited-state consists almost entirely of basis states in which one electron is excited and the other remains unperturbed in the Na atom 3s orbital.[47] Given that the solvent interacts quite differently with these two electrons after excitation, we expect that rapid solvent-induced dephasing will remove any memory of the correlation between the two electrons soon after CTTS excitation.[48] Thus, to a high degree of accuracy, CTTS excitation can be thought of as promoting one of the two 3s electrons on sodide into a solvent-bound p-like excited state, while the second electron is left alone on the sodium atom core. We can then probe the CTTS excited state spectroscopically by monitoring either the electronic absorption of the excited electron in the near-IR between 1200 and 1500 nm or the core absorption of the remaining 3s electron at 590 nm.

Our understanding of the nature of the CTTS transition also provides a means to anticipate the results of future polarization-dependent transient absorption experiments. We expect that experiments with better time resolution than our own would reveal a measurable, although rapidly decaying, *negative* polarization anisotropy of ~1250 nm excited-state absorption. This is because the local solvent asymmetry that splits the degeneracy of the three p-like CTTS excited states has a preferential spatial orientation. As long as solvation dynamics do not destroy memory of this spatial orientation, the p-to-p excited-state absorption should be orthogonally polarized to the initial CTTS excitation, giving rise to a negative anisotropy. The valence electron that remains in the 3s orbital on the Na atom core, in contrast, is not affected by the local solvent asymmetry: the fact that the electronic absorption of this electron occurs at the same spectral position as in the gas phase verifies that interactions with the surrounding solvent are minimal. Thus, we would expect the 590 nm absorption to carry no memory of the excitation

polarization, exactly as observed by Ruhman and co-workers.[18] Overall, whether or not our predicted negative anisotropy of the 1250 nm band can be observed, the fact that both the 1250 nm and 590 nm early-time absorption features appear universally across multiple solvents[49] supports the idea that both are affiliated with the unsolvated CTTS excited state.

D. Solvent polarity and the recombination of solvent-separated contact pairs

Having presented a rationalization of the behavior of the earliest-time features in the transient absorption spectroscopy of sodide, we turn next to a discussion of the long time (>10 ps) features shown in Fig. 6. As we have argued above, the newly detached CTTS electron can localize at various distances from its geminate sodium atom partner, depending upon the excitation energy.[13,14] For higher excitation energies, we believe that a significant number of electrons localize one solvent shell away from their geminate Na^0 partners, in solvent-separated contact pairs. These contact pairs should be metastable entities;[13,14] their back electron transfer takes place on a hundreds-of-picoseconds time scale, as reflected by the decay of the 2 μm solvated electron absorption on this time scale in Fig. 6. The metastable nature of these pairs is supported by both simulation work from Staib and Borgis, who found a minimum in the potential of mean force for electrons ejected from aqueous chloride,[11] and experimental work from Bradforth and co-workers, who have successfully modeled the recombination of electrons following CTTS detachment from aqueous iodide using diffusion over a potential barrier.[1] In the DE+S model, we account for the recombination of solvent-separated contact pair electrons in Eqs. (7)–(9), although we have not yet considered this recombination process in detail pending more information on the nature of the barrier from our quantum simulations.[50] Thus, in this section, we turn to a qualitative discussion of the nature of the long-time back electron transfer.

One of the things apparent from Figs. 3–5 is that the fraction of electrons that localize into solvent-separated contact pairs (i.e., the height of the offsets in the pump–probe scans) differs between solvents, even when similar excitation wavelengths were used [e.g., Figs. 3(Q), 4(C), 4(F), and 5(A)]. We believe that this results from differences in local solvent structure that determine the ease of detachment into immediate versus solvent-separated contact pairs, as we will discuss further below. Figure 6 indicates that the long-time back electron transfer following $\sim$490 nm CTTS excitation of Na^- is much faster in DEE than in THF or THP. Even more remarkable is the fact that the temporal evolution in HMPA is essentially flat on the subnanosecond time scale: after the early time spectral dynamics are complete, there appears to be no recombination of solvent-separated contact pairs in this solvent. Thus, the stability of the solvent-separated contact pairs appears to scale with solvent polarity (cf. Tables I and II): the more polar the solvent, the slower the rate of solvent-separated contact pair back electron transfer.

To explain these differences in long-time recombination behavior, we propose that the solvent structure surrounding the solvent-separated contact pair provides progressively less stabilization as the solvent polarity decreases: the less polar the solvent, the less stable the contact pair. This results in a lower free energy barrier for back electron transfer and thus more rapid recombination. For the most polar solvent studied, HMPA, we expect that the solvent-separated contact pairs will be better solvated and thus more stable than in any of the ethers. In the language of Marcus theory,[7,13] we would argue that the back electron transfer of solvent-separated pairs lies in the inverted regime: increasing the polarity of the solvent stabilizes the Na^- product of the back electron transfer and thus increases the driving force for recombination, but increasing polarity also increases the height of the barrier that must be overcome for recombination to take place.[51] We are presently conducting temperature-dependent pump–probe experiments on Na^- in different solvents in an effort to determine the barrier height for the solvent-separated contact pair back electron transfer process.

E. Electron localization and the recombination of immediate contact pairs

In addition to the production of solvent-separated contact pairs, CTTS excitation of sodide also can lead to electron detachment into the same solvent cavity as the parent sodium atom. The recombination times for immediate contact pairs are much faster ($\sim$1 ps) than those for solvent-separated contact pairs (tens to hundreds of picoseconds); the experimental evidence for this fast recombination was presented above in Sec. III A. Table II, column 3 shows that for the three ethers, the back ET times for immediate contact pairs (τ_2 in the DE+S model) decrease with increasing solvent polarity, the opposite of what we observed for the back ET times of solvent-separated pairs. In addition, the polarity trend for the recombination of immediate contact pairs does not hold in HMPA: the recombination of immediate contact pairs in HMPA takes $\sim$2.5 ps, significantly longer than the $\sim$1 ps recombination observed in the ethers.

We can rationalize the trend in immediate-pair recombination times with solvent using the fact that the spatial extent of the solvated electron is different in each solvent. Our idea is based on recent work by Barbara and co-workers, who have determined that the probability for a solvated electron to react with a nearby scavenger is proportional to the electron density in contact with the scavenger.[52,53] Thus, it is the overlap of the solvated electron's wave function with the vacant 3*s* orbital on the Na atom that should determine the rate of immediate-pair back electron transfer. The electron density in contact with the Na atom in turn depends on the degree of localization of the solvated electron. Thus, we would expect the back ET times to correlate with the spatial extent of the electron in each solvent environment. For example, in THF, the most polar ether studied, we expect electrons to be more localized than their counterparts in the less polar ethers. The more localized electron in THF has greater wave function overlap with the Na atom in its first solvent shell than the less localized electrons in the other ethers,

leading to a higher back electron transfer rate (lower recombination time τ_2) in THF.

While the general trend is that less polar solvents provide less spatial localization for solvated electrons, HMPA is an exception. It is known that liquid HMPA is characterized by large voids that result from difficulties with close packing of the relatively bulky HMPA solvent molecules.[29] Thus, even though HMPA is a highly polar solvent, the spatial extent of the solvated electron in this solvent is quite large: this explains why the solvated electron in this solvent has its absorption maximum to the red of 2 μm instead of closer to the visible as with other amines.[29] We will argue below in Sec. IV F that the CTTS detachment of electrons from Na^- in HMPA is enhanced because the pre-existing voids provide stabilization for the electron without significant solvent motion. The increased spatial extent of the electron in these voids (relative to the ethers) is what lowers the immediate-pair back electron transfer rate: upon ejection, the electron is so delocalized that it has relatively little direct overlap with the nearby sodium atom. Overall, the time for the recombination of immediate contact pairs appears to scale with the spatial extent of the electron in each of the various solvents.

F. The role of solvent structure and dynamics in CTTS electron detachment

Although trends with the degree of electron localization and solvent polarity can explain the back electron transfer times for immediate and solvent-separated contact pairs, simple bulk solvent properties do not appear to be the most important factors in determining the forward electron transfer (CTTS detachment) dynamics. The variation in CTTS detachment time (τ_1) with solvent does not correlate simply with any of the bulk solvent characteristics summarized in Table I. In previous work, we postulated that translational motions of a few of the first-shell solvent molecules into the angular node of the *p*-like CTTS excited-state wave function are primarily responsible for the detachment of the electron into its more *s*-like equilibrium structure in an immediate or solvent-separated contact pair.[54] Thus, we expect that the rate of CTTS detachment correlates with how well a given solvent's structure and dynamics promote or retard the requisite first-shell translational motions.

Of the ethers, the CTTS detachment of electrons from Na^- is the fastest in THF. THF is a nearly planar, disk-like molecule, and Monte Carlo simulations suggest that the structure of liquid THF involves stacks of parallel molecules.[55] Preliminary results from MD simulations of THF underway in our group[56] indicate coupling between center-of-mass translations and spinning (around an axis normal to the plane) of the THF ring. Since we believe the primary factors in CTTS ejection involve solvent translations that respond to the CTTS excitation and create the cavity into which the electron detaches, this type of translation-rotation coupling should help promote rapid electron ejection.[57] DEE, the solvent with the next-fastest Na^- CTTS ejection time, is quite similar in structure to THF, but has free rotations around the C–O bonds. These rotations should produce a more disordered solvent structure for DEE than THF (i.e., the formation of stacks of molecules is less likely), so that it takes longer for solvent translations to respond to CTTS excitation or create a cavity for the detached electron. Finally, the structure of THP is quite similar to that of cyclohexane, in which the molecules form ''chairlike'' structures that stack well in the liquid.[58] We believe that this stacking significantly slows local translational motions (since the molecules must ''unstack'' before they are able to undergo translational rearrangement), leading to the slowest CTTS detachment time among the three ethers. Although these ideas are speculative, it makes sense that the most important factors regulating CTTS detachment depend on the local solvent molecular structure rather than bulk liquid parameters.

Our ideas about local solvent structure determining the forward CTTS detachment rate also can be used to rationalize the fact that electrons appear to be ejected more quickly in HMPA than in the ethers. One would expect that the translational motions of HMPA should be slower than those in the ethers given both the size and mass of the HMPA molecule. We already have pointed out, however, that HMPA has an unusual solvent structure that contains many pre-existing voids.[29] We expect that these voids act as stable traps for the excited CTTS electron, allowing detachment to take place faster than in the more tightly packed ethers where significant local rearrangement is required to produce the electron's cavity. One caveat concerning this argument is that our experimental evidence that CTTS ejection is faster in HMPA than in the ethers comes only from scans probing at 2 μm: we do not have the corresponding scans in the visible to constrain the fitting procedure and confirm the fast detachment time. Our arguments in Sec. IV A suggest that the CTTS excited state should present an instrument-limited absorption at 2 μm as well as the one near 1250 nm discussed in Sec. IV A;[40] thus, it is difficult to extract cleanly the detachment time in HMPA from the data in Fig. 4. Whether or not the 2 μm data consists of an instrument-limited rise due to the excited state absorption plus slower rise due to detachment or only a single rise, the fast appearance of electrons in HMPA suggests that the local solvent structure is the most important factor in controlling CTTS detachment dynamics.

G. Solvation dynamics of the CTTS-created sodium atom

In addition to the forward and reverse electron transfer rates, the data in Figs. 3–5 also contain information about the time-dependent solvation dynamics that shift the spectrum of the neutral Na atom. In the DE+S model, we describe this spectrum as a combination of Gaussian low-energy and Lorentzian high-energy halves, as discussed further in Ref. 31. The parameters that account for the shift are the time-zero half-widths of the Gaussian and Lorentzian parts of the Na^0 spectrum, the peak absorption wavelength, and the integrated area under the band. Each of these parameters evolves as prescribed in the SI [Eqs. (S7)–(S9)] until the steady-state Na^0 spectrum[19] is achieved. As explained in detail in Ref. 31, the time-dependent Na^0 spectrum shifts in energy and broadens with time t_1 and grows in oscillator strength with time t_2, as summarized in Table II. Given that the solvent was equilibrated for the anionic ground state and must reorient to stably solvate the neutral sodium following

CTTS ejection, we expect that these solvation times should be similar to the relaxation times measured in these solvents in time-dependent Stokes shift experiments.[59,60]

This expectation appears to be born out in THF, for which the longer dielectric solvation time is known to be 1.5 ps,[59] in good agreement with our fitted spectral shifting time t_1 of 1.4 ps. The time required for the area of the spectrum to change with solvation (t_2), however, is 2.4 ps, which is slower than literature values for dielectric solvation in this fluid. A similar 2.4 ps solvation time constant also has been observed by Ruhman and co-workers in this system,[18] suggesting that some type of additional solvent response, possibly a mechanical or viscoelastic relaxation,[61] is necessary to reach equilibrium following CTTS excitation. To the best of our knowledge, time-dependent Stokes shift experiments have not been performed in either DEE or THP, so we are unable to make this same type of comparison for the solvation shifting times of Na^0 in these two solvents. We also cannot make this comparison for HMPA, even though the Stokes shift data are available,[60] because our limited data set in HMPA prevents us from extracting the sodium atom solvation times in this solvent.[22]

V. CONCLUSIONS

In summary, study of the sodide CTTS system in different solvents has provided detailed information about how solvent motions and liquid structure determine the rates of electron transfer reactions. We found that the rate at which an electron detaches from the Na^- CTTS excited state depends primarily on the local solvent structure around the anion; the solvents whose first-shell molecules are more able to undergo translational motions have faster CTTS detachment times. For the back ET reactions that regenerate Na^-, the solvated electrons in immediate pairs recombine faster when their wave functions are more localized, resulting in improved overlap with the 3*s* wave function of their geminate Na^0 partners. Electrons in solvent-separated contact pairs, on the other hand, have increasingly stable solvation structures and move farther into the Marcus inverted regime in more polar solvents, resulting in a direct correlation between the survival time of the solvent-separated contact pair and solvent polarity. Because each process in the CTTS reaction depends on the solvent in a different way, it is clear that one spectral density or set of solvent motions cannot describe all aspects of these types of processes.

To gain better insight into the complex nature of all these processes, we refined our previous model for the CTTS dynamics of the Na^- system. The DE+S model has all the features of our previous ''delayed ejection'' model:[13] instantaneous creation of a CTTS excited state that has a $\sim$590 nm D-line-like absorption spectrum, detachment of the electron in $\sim$700 fs (in THF) to produce a distribution of Na^0:e^- contact pairs, followed by recombination of the various contact pairs to regenerate ground state Na^-. The new feature introduced here is a kinetic means to model the dynamic solvation shift of the Na^0 species, which in THF takes place on roughly the same time scale observed in time-dependent Stokes shift experiments. The fact that this model is able to describe data taken in other solvents (DEE, THP, and HMPA) strongly suggests that it has correctly captured the underlying physics of the CTTS detachment and recombination processes. Furthermore, it was straightforward to add anisotropic bleaching dynamics to the model, allowing us to explain polarized pump–probe scans without the need for invoking additional processes such as stimulated emission. We also were able to account for the rapidly decaying absorption feature near 1250 nm as the direct absorption and subsequent solvation of the CTTS excited state. Overall, we believe that our basic picture of this model electron transfer reaction is correct,[13] although refinements such as the effects of solvation on the spectra of other species may need to be incorporated to obtain a full quantitative description of this reaction.

The fact that the DE+S model can successfully describe the data in multiple solvents led us to perform a detailed comparison of the interpretations of both our group and that of Ruhman and co-workers concerning the assignment of the fastest dynamics in the transient spectroscopy of Na^- in THF. While we associate the $\sim$200 fs features seen at 850 and $\sim$1200 nm to solvent dynamics that affect the anisotropic bleach and the weakly allowed $p \rightarrow p$ excited-state absorption, respectively, Ruhman and co-workers assign these features to population dynamics that alter stimulated emission and absorption from the CTTS excited state.[18] Ruhman and co-workers interpretation also requires that both Na^- valence electrons, in sequence, are ejected following CTTS excitation.[18] While this second electron ejection is certainly possible, we feel that the data for this system can be explained satisfactorily without invoking such a complex process: we do not believe that a three-body recombination event could force both electrons back onto a Na^+ within a ps (or within 200 fs after re-excitation of one of the electrons[15]). Moreover, any kinetic model based on the ideas of Ruhman and co-workers would have to have a large number of adjustable parameters; in addition to the same parameters needed for our DE+S model, a scheme based on Ruhman and co-workers picture also would need to include separate time constants for the ejection and solvation of the second electron, plus three-body equations with rate constants for all the possible recombination processes. Given the relative simplicity of the DE+S model and the fact that (with the addition of a single parameter to describe spectral diffusion in the polarized transient bleach) it is consistent with *all* the data presented by both our group and Ruhman's, we believe that it represents the best choice for interpreting the underlying molecular physics associated with CTTS in this system.

ACKNOWLEDGMENTS

We thank Ross E. Larsen for useful discussions concerning anisotropic bleaching dynamics and the quantum mechanics of two-electron systems, and Sandy Ruhman and Roseanne Sension for stimulating discussions concerning the nature of the Na^- CTTS reaction and for sharing results prior to publication. This work was supported by the National Science Foundation under CAREER Award CHE-9733218, and the NSF–OTKA joint project 38455. B.J.S. is

a Cottrell Scholar of Research Corporation, an Alfred P. Sloan Foundation Research Fellow, and a Camille Dreyfus Teacher-Scholar.

[1] V. H. Vilchiz, J. A. Kloepfer, A. C. Germaine, V. A. Lenchenkov, and S. E. Bradforth, J. Phys. Chem. A **105**, 1711 (2001); J. A. Kloepfer, V. H. Vilchiz, V. A. Lenchenkov, A. C. Germaine, and S. E. Bradforth, J. Chem. Phys. **113**, 6288 (2000); J. A. Kloepfer, V. H. Vilchiz, V. A. Lenchenkov, and S. E. Bradforth, Chem. Phys. Lett. **298**, 120 (1998).

[2] L. Lehr, M. T. Zanni, C. Frischkorn, R. Weinkauf, and D. M. Neumark, Science **284**, 635 (1999); A. V. Davis, M. T. Zanni, C. Frischkorn, and D. M. Neumark, J. Electron Spectrosc. Relat. Phenom. **108**, 203 (2000); M. T. Zanni, C. Frischkorn, A. V. Davis, and D. M. Neumark, J. Phys. Chem. A **104**, 2527 (2000); A. V. Davis, M. T. Zanni, R. Weinkauf, and D. M. Neumark, Chem. Phys. Lett. **353**, 455 (2002).

[3] F. H. Long, X. Shi, H. Lu, and K. B. Eisenthal, J. Phys. Chem. **98**, 7252 (1994); F. H. Long, H. Lu, X. Shi, and K. B. Eisenthal, Chem. Phys. Lett. **169**, 165 (1990); F. H. Long, H. Lu, and K. B. Eisenthal, J. Chem. Phys. **91**, 4413 (1989).

[4] Y. Gauduel, M. Sander, and H. Gelabert, J. Mol. Liq. **78**, 111 (1998); H. Gelabert and Y. Gauduel, J. Phys. Chem. **100**, 13993 (1996); Y. Gauduel, H. Gelabert, and M. Ashokkumar, Chem. Phys. **197**, 167 (1995); Y. Gauduel, H. Gelabert, and M. Ashokkumar, J. Mol. Liq. **64**, 57 (1995).

[5] See, e.g., F. H. Long, H. Lu, X. Shi, and K. B. Eisenthal, Chem. Phys. Lett. **185**, 47 (1991); S. Pommeret, A. Antonetti, and Y. Gauduel, J. Am. Chem. Soc. **113**, 9105 (1991); R. Laenen, T. Roth, and A. Laubereau, Phys. Rev. Lett. **85**, 50 (2000); A. Hertwig, H. Hippler, A. N. Unterreiner, and P. Vöhringer, Ber. Bunsenges. Phys. Chem. **102**, 805 (1998); J. L. McGowen, H. M. Ajo, J. Z. Zhang, and B. J. Schwartz, Chem. Phys. Lett. **231**, 504 (1994); C. L. Thomsen, D. Madsen, S. R. Keiding, and J. Thøgersen, J. Chem. Phys. **110**, 3453 (1999); C. Pepin, D. Houde, H. Remita, T. Goulet, and J.-P. Gerin, J. Phys. Chem. A **101**, 4351 (1997); M. U. Sander, U. Brummund, K. Luther, and J. Troe, J. Phys. Chem. **97**, 8378 (1993); Y. Hirata and N. Mataga, *ibid.* **95**, 1640 (1991); D. M. Bartels and R. A. Crowell, J. Phys. Chem. A **104**, 3349 (2000).

[6] M. J. Blandamer and M. F. Fox, Chem. Rev. **70**, 59 (1970).

[7] R. A. Marcus and N. Sutin, Biochim. Biophys. Acta **811**, 265 (1985); P. F. Barbara, T. J. Meyer, and M. A. Ratner, J. Phys. Chem. **100**, 13148 (1996).

[8] H. Y. Chen and W.-S. Sheu, J. Am. Chem. Soc. **122**, 7534 (2000); Chem. Phys. Lett. **335**, 475 (2001); **353**, 459 (2002).

[9] S. E. Bradforth and P. Jungwirth, J. Phys. Chem. A **106**, 1286 (2002).

[10] W.-S. Sheu and P. J. Rossky, J. Phys. Chem. **100**, 1295 (1996); J. Am. Chem. Soc. **115**, 7729 (1993); Chem. Phys. Lett. **213**, 233 (1993); **202**, 186 (1993).

[11] A. Staib and D. Borgis, J. Chem. Phys. **103**, 2642 (1995); **104**, 9027 (1996); **104**, 4776 (1996).

[12] M. Maroncelli, J. Mol. Liq. **57**, 1 (1993); G. R. Fleming and M. Cho, Annu. Rev. Phys. Chem. **47**, 109 (1996); P. J. Rossky and J. D. Simon, Nature (London) **370**, 263 (1994); W. P. DeBoeij, M. S. Pshenichnikov, and D. A. Wiersma, Annu. Rev. Phys. Chem. **49**, 99 (1998); J. T. Hynes, in *Ultrafast Dynamics of Chemical Systems*, edited by J. D. Simon (Kluwer, Dodrecht, 1994), p. 345.

[13] E. R. Barthel, I. B. Martini, and B. J. Schwartz, J. Phys. Chem. B **105**, 12230 (2001).

[14] I. B. Martini, E. R. Barthel, and B. J. Schwartz, J. Chem. Phys. **113**, 11245 (2000); E. R. Barthel, I. B. Martini, and B. J. Schwartz, *ibid.* **112**, 9433 (2000).

[15] I. B. Martini, E. R. Barthel, and B. J. Schwartz, J. Am. Chem. Soc. **124**, 7622 (2002); Science **293**, 462 (2001); I. B. Martini and B. J. Schwartz, Chem. Phys. Lett. **360**, 22 (2002).

[16] J. L. Dye, J. Phys. Chem. **84**, 1084 (1980); J. Chem. Educ. **54**, 332 (1977); M. T. Lok, F. J. Tehan, and J. L. Dye, J. Phys. Chem. **76**, 2975 (1972).

[17] Z. Wang, O. Shoshana, and S. Ruhman, *Ultrafast Phenomena XII*, Springer Series in Chemical Physics (Springer-Verlag, Heidelberg, 2001), p. 624.

[18] R. Sension, Z. Wang, O. Shoshana, B. Hou, and S. Ruhman, *Ultrafast Phenomena XIII*, Springer Series in Chemical Physics (Springer-Verlag, Heidelberg, 2002); Z. Wang, O. Shoshana, B. Hou, and S. Ruhman (unpublished); R. Sension and S. Ruhman (private communication).

[19] Although we have reassigned the 900 nm absorbing species to solvated Na^0 (Refs. 13 and 14) this species was originally assigned as a sodium cation:solvated electron contact pair (the idea is that the presence of the nearby Na^+ shifts the $\sim 2\ \mu$m absorption of the solvated electron all the way to $\sim$900 nm). See, e.g., P. Piotrowiak and J. R. Miller, J. Am. Chem. Soc. **113**, 5086 (1991); B. Bockrath and L. M. Dorfman, J. Phys. Chem. **79**, 1509 (1975); **77**, 1002 (1973).

[20] The solvent dynamics underlying many chemical reactions and/or nonlinear optical experiments are often expressed in terms of a Brownian Oscillator model that accounts for the affects of the bath using a single spectral density. See, e.g., S. Mukamel, *Principles of Non-Linear Optical Spectroscopy* (Oxford University Press, London, 1995).

[21] We note that solutions prepared in THP and DEE were considerably less stable than those prepared in THF; this required the use of more concentrated solutions for pump–probe measurements. Due to instrumental limitations in the choice of pump and probe wavelengths (see Ref. 25) and the high optical density of these samples at visible wavelengths, the wavelength ranges in which data could be obtained in THP and DEE were limited relative to the less concentrated, more stable THF samples.

[22] Typically, the optical density of our 0.1 mm Na^-/HMPA samples was $\sim$3 at 750 nm. Because of this and the instability of these solutions, visible probe experiments could not be performed reliably. See Ref. 21 for similar concerns regarding THP and DEE solutions.

[23] J. M. Brooks and R. R. Dewald, J. Phys. Chem. **72**, 2655 (1968).

[24] T.-Q. Nguyen, I. B. Martini, J. Liu, and B. J. Schwartz, J. Phys. Chem. B **104**, 237 (2000).

[25] As pointed out in Refs. 21 and 22, the optical density of our Na^- samples in solvents other than THF is typically $\geqslant$2.5 near the absorption maximum. This means that low-energy light pulses, such as those obtained by continuum generation, cannot penetrate the sample and be detected with a sufficient signal-to-noise ratio. Thus, we used sum-frequency generation of the 780 nm fundamental with the OPA signal or idler beams to generate higher-energy (typically a few tens to a few hundred nJ) probe pulses for visible-probe experiments. Since the pump pulse was also generated by sum-frequency of the 780 nm fundamental with the OPA idler or signal beams, the choice of pump and probe wavelength combinations available for our visible-probe experiments was limited. (This is because the OPA signal and idler wavelengths are coupled, in that the sum of the OPA signal and idler photon energies must match that of the 780 nm fundamental). Our choice of probe wavelengths also was limited by the tuning range of our OPA, which can only produce signal beams between 1150 and 1500 nm without substantial loss of stability and signal-to-noise. The data shown in Fig. 9 are an exception, obtained by using an aged Na^-/THP sample that degraded significantly during the several days of data collection necessary for signal averaging.

[26] C. Laurence, P. Nicolet, M. T. Dalati, J.-L. M. Abboud, and R. Notario, J. Phys. Chem. **98**, 5807 (1994).

[27] *CRC Handbook of Chemistry and Physics*, 3rd electronic ed. (Chemical Rubber Company, Boca Raton, FL, 2000), http://www.knovel.com/knovel2/Toc.jsp?SpaceID=10093&BookID=34

[28] S. Rodriguez, C. Lafuente, P. Cea, F. M. Royo, and J. S. Urieta, J. Chem. Eng. Data **42**, 1285 (1997).

[29] E. A. Shaede, L. M. Dorfman, G. F. Flynn, and D. C. Walker, Can. J. Chem. **51**, 3905 (1973).

[30] L. M. Dorfman, F. Y. Jou, and R. Wageman, Ber. Bunsenges. Phys. Chem. **75**, 681 (1971); F. Y. Jou and L. M. Dorfman, J. Chem. Phys. **58**, 4715 (1973); F. Y. Jou and G. R. Freeman, Can. J. Chem. **54**, 3693 (1973).

[31] See EPAPS Document No. E-JCPSA6-118-511313 for details of the implementation of the DE+S model, details of the extension to include polarized hole-burning, and an Excel spreadsheet that allows simulation of polarized transient absorption data for Na^- in THF at any pump and probe wavelength combinations. A direct link to this document may be found in the online article's HTML reference section. The document may also be reached via the EPAPS homepage (http://www.aip.org/pubservs/epaps.html) or from ftp.aip.org in the directory /epaps/. See the EPAPS homepage for more information.

[32] Fletcher and Seddon [J. W. Fletcher and W. A. Seddon, J. Phys. Chem. **79**, 3055 (1975)] found no spectroscopic signatures for Na^0 in DEE and surmised that this species must absorb at the same wavelength as Na^- in this solvent. We note, however, that the time resolution of their pulse radiolysis setup was $\sim 1\ \mu$s, and Fig. 6 shows that there is significant recombination of solvated electrons with the Na^0 in DEE well within this time. Thus, we believe that using the Na^0 spectral parameters from THF is a reasonable approximation to the true short-time Na^0 spectrum in the other ether solvents.

[33] We note that there is some uncertainty in the literature concerning the value of the molar extinction coefficient of the solvated electron; see, e.g.,

the first two papers of Ref. 30. However, variations in the electron's absolute absorbance do not strongly affect the estimated values of the parameters in our model. The only spectral region in which the solvated electron's absorption is significant relative to the other species is 1100–1500 nm, where the Na^0 and Na^{-}* also absorb.

[34] L. Turi, P. Holpár, and E. Keszei, J. Phys. Chem. A **101**, 5469 (1997); E. Keszei, T. H. Murphrey, and P. J. Rossky, J. Chem. Phys. **99**, 22 (1995).

[35] D. W. Marquardt, J. Soc. Ind. Appl. Math. **11**, 431 (1963).

[36] Scans using a 780 nm excitation wavelength require an adjustable recombination fraction p due to two-photon absorption that changes the fraction of electrons ejected into immediate and solvent-separated contact pairs; see the first paper of Ref. 14 for details.

[37] The DE model we presented previously also is capable of fitting the data in Figs. 3 and 4, and is even more highly constrained than the DE+S model because it has fewer parameters since the shifting of the Na^0 spectrum is not described. However, we believe that the additional parameters needed to describe the solvation dynamics in the DE+S model are justified because a considerably better agreement with the measured data is obtained, particularly for the visible probe wavelengths close to the ~880 nm peak of the Na^0 absorption.

[38] B. J. Schwartz and P. J. Rossky, Phys. Rev. Lett. **72**, 3282 (1994).

[39] P. J. Rossky and J. Schnitker, J. Phys. Chem. **92**, 4277 (1988).

[40] Based on this picture we would also expect the center-to-highest p-to-p transition to absorb in the ~2 μm range, explaining a small instrument-limited component that precedes the delayed rise due to electron detachment.

[41] As indicated by the y axis of Fig. 8, we can estimate the molar absorption cross section of this species by comparing to the subsequent absorption rise from electron/Na^0, and it is indeed quite small, only a few thousand L mol^{-1} cm^{-1}. We note that the absolute value calculated for the Na^{-}* p-to-p cross section depends on our assumed value for the absorbance of the solvated electron in this spectral region, which is itself uncertain; see Ref. 33.

[42] As described in B. J. Schwartz and P. J. Rossky, J. Chem. Phys. **101**, 6917 (1994), the excited-state absorption of the hydrated electron changes dramatically as the solvent moves to stabilize the newly created p-like excited state, breaking the symmetry and changing both the energy and oscillator strength of the p-to-p absorption. We expect the CTTS excited state of Na^{-} to show a similar sensitivity to solvent motions, as emphasized in Fig. 8.

[43] J. Yu and M. Berg, J. Phys. Chem. **97**, 1758 (1993).

[44] The differences in time scale in Fig. 9 between the experiments and the model are the result of a small two-photon absorption component in the experiments that is not included in the simulations (cf. Ref. 36). We believe, however, that this two-photon component does not strongly influence the anisotropic spectral dynamics since two-photon absorption should result in excitation to the Na^{-} detachment continuum, which should have no polarization memory.

[45] The fact that we needed to adjust the blue-side probe wavelength to reproduce the polarized pump–probe data suggests that our crude fit of the absorption spectrum to a simple sum of Gaussians is somewhat in error. Most likely, the individual sub-bands have a more complex line shape, so that the crossing point of the two lowest-energy bands is nearer to 720 nm rather than to 670 nm as predicted by the model. The crossing point might also be bluer than expected because of differences in the structure of the equilibrium CTTS absorption spectrum of Na^{-} between THF and THP.

[46] To us, the major difficulty with Ruhman and co-workers' assignment of the 590 nm feature to an unsolvated ''hot'' sodium atom produced after detachment is that this assignment cannot explain why the appearance time of this feature is instrument limited, even at Ruhman and co-workers' high time resolution. We also do not believe that the solvent could have responded to a degree sufficient to detach the electron without providing any solvation of the Na atom core.

[47] R. E. Larsen and B. J. Schwartz (in preparation).

[48] We believe that there should be very rapid dephasing of the solvent-supported CTTS electronic excited state, as also has been seen for the solvent-supported excited state of the hydrated electron; see, e.g., A. Baltushka, M. F. Emde, M. S. Pshenichnikov, and D. A. Wiersma, J. Phys. Chem. A **103**, 10065 (1999); S. J. Rosenthal, B. J. Schwartz, and P. J. Rossky, Chem. Phys. Lett. **229**, 443 (1994); O. V. Prezhdo and P. J. Rossky, Phys. Rev. Lett. **81**, 5294 (1998). Ruhman and co-workers, in contrast, believe that electronic dephasing does not occur until the electron is ejected (Ref. 18).

[49] In E. R. Barthel, I. B. Martini, E. Keszei, and B. J. Schwartz, in *Ultrafast Phenomena XIII*, Springer Series in Chemical Physics (Springer-Verlag, Heidelberg, 2002), we show that the Na^{-}* spectrum is identical in the three ethers within the precision of the DE+S fits to the data.

[50] C. J. Smallwood, W. B. Bosma, R. E. Larsen, and B. J. Schwartz (in preparation).

[51] Kohler and co-workers have seen a similar result for the recombination of hydrated electrons with aqueous indole radical cation, see J. Peon, G. C. Hess, J. M. L. Pecourt, T. Yuzawa, and B. Kohler, J. Phys. Chem. A **103**, 2460 (1999).

[52] P. Kambhampati, D. H. Son, T. W. Kee, and P. F. Barbara, J. Phys. Chem. A **106**, 2374 (2002); T. W. Kee, D. H. Son, P. Kambhampati, and P. F. Barbara, *ibid.* **105**, 8434 (2001); D. H. Son, P. Kambhampati, T. W. Kee, and P. F. Barbara, *ibid.* **105**, 8269 (2001).

[53] This idea is also consistent with our work showing control over the back electron transfer of Na^0: solvated electron contact pairs by changing the electron density of the solvated electron using a sequence of femtosecond laser pulses; see Ref. 15.

[54] This is also analogous with the solvation dynamics of the photoexcited hydrated electron. See, e.g., B. J. Schwartz and P. J. Rossky, J. Chem. Phys. **101**, 6902 (1994).

[55] J. Chandrasekhar and W. L. Jorgensen, J. Chem. Phys. **77**, 5073 (1982).

[56] M. Bedard-Hearn, R. E. Larsen, and B. J. Schwartz (in preparation).

[57] This type of translation–rotation coupling also has been observed in molecular dynamics simulations of solvation dynamics following changes in the size and shape of spherical solutes; see D. Aherne, V. Tran, and B. J. Schwartz, J. Phys. Chem. B **104**, 5382 (2000).

[58] J. G. Harris and F. H. Stillinger, J. Chem. Phys. **95**, 5953 (1991).

[59] L. Reynolds, J. A. Gardecki, S. J. V. Frankland, M. L. Horng, and M. Maroncelli, J. Phys. Chem. **100**, 10337 (1996).

[60] M. L. Horng, J. A. Gardecki, A. Papazyan, and M. Maroncelli, J. Phys. Chem. **99**, 17311 (1995).

[61] M. Berg, J. Chem. Phys. **110**, 8577 (1999); J. Phys. Chem. A **102**, 17 (1998); S. Bhattacharya and B. Bagchi, J. Chem. Phys. **109**, 7885 (1998); M. Berg, Chem. Phys. Lett. **228**, 317 (1994); **228**, 317 (1994).